Electronic states above a helium film suspended on a ring-shaped substrate

A. C. A. Ramos,* A. Chaves,† and G. A. Farias‡
Departamento de Física, Centro de Ciências Exatas, Universidade Federal do Ceará, Campus do Pici, Caixa Postal 6030, 60455-760 Fortaleza, Ceará, Brazil

F. M. Peeters§
Departament of Physics, University of Antwerp (CGB), Groenenborgerlaan 171, B-2020 Antwerp, Belgium
(Received 7 August 2007; published 18 January 2008)

We derived a nonlinear differential equation that describes the profile of a suspended helium film over a ring-shaped substrate in the presence of a perpendicular external electric field. The profile of the helium film was calculated as a function of the bulk liquid helium level and for several values of the external radius of the ring. The one electron surface states were calculated in the presence of external electric and magnetic fields. The electron energy levels increase with electric field as well as with the height of bulk helium. Aharonov-Bohm oscillations were observed in this system under appropriate conditions.

DOI: 10.1103/PhysRevB.77.045415 PACS number(s): 73.20.−r

I. INTRODUCTION

Since the first works of Sommer,[1] Cole and Cohen,[2] and Shikin,[3] the study of surface states of electrons bounded to the surface of liquid helium has been the subject of many studies.[4,5]

The progress in nanofabrication of semiconductor materials allowed the construction of quantum wires and a new confined structure called quantum rings (QRs). The semiconductors materials, QRs, are modeled by a cylindrical quantum dot with an internal axially symmetric cavity. This unique geometry has attracted much attention in the last few years.[6–8] Although the new techniques of building new semiconductor structures improved considerably in the last few years, the electron properties are strongly influenced by spatial inhomogeneities and impurity scattering.[9–11] The uniformity and cleanliness of electron systems on a helium surface have proved to be practically ideal for experimental and theoretical research on low-dimensional systems. Taking into account these studies on low-dimensional systems devoted to quantum wires and quantum dots in semiconductor devices, it would be natural to study similar systems of electrons above a helium surface in quasi-one-dimensional (Q1D) and quasi-zero-dimensional structures (see review[12]). The physical realization of Q1D electron systems over liquid helium allowed us to study different phenomena, such as transport properties, plasmons, and polaronic states.[12–14] In these systems, the charge carriers can move only in one spatial direction due to lateral confinement. Such confinement leads to a lateral potential introducing a new spatial quantization leading to a multisubband electron system. Considering a parabolic lateral confinement, Sokolov and Studart[15] studied the effects of a transverse magnetic field on the electron states in a Q1D electron system over liquid helium. Recently, the profile of the suspended helium film, forming a channel, was calculated self-consistently. It was shown that, under certain experimental conditions reported in the literature,[14] the lateral potential can be approximated by a parabolic potential.[16] In fact, a very efficient way to produce Q1D electron systems over liquid helium is the technique of suspended helium film on a structured substrate. Compared to a thin van der Waals film, a suspended helium film has the advantage of being much thicker and therefore less sensitive to the roughness of the substrate beneath it. This improves the mobility of the electrons on the film.[17] Furthermore, since the suspended helium film follows the substrate shape, it opens up the possibility to create one-dimensional channels by suspending a film between ribs, zero-dimensional structures by making (small) holes in a flat substrate, and even rings.

The QR is usually modeled by a cylindrical quantum dot with an internal axially symmetric cavity. This unique geometry has attracted much attention in the last few years.[6–10,18–22] In the presence of an axially directed magnetic field, oscillations of the electron energy as a function of the magnetic flux [Aharonov-Bohm effect (ABE)] were found to occur.[23] The AB oscillations are due to a change of phase of the wave function when the magnetic flux ϕ passing through the ring reaches the magnetic quantum flux $\phi_0 = h/e$ (h is the Planck constant and e is the electronic charge). As expected for semiconductor structures, some works have pointed out that the presence of impurities and geometrical imperfections affect strongly the optical properties and the electronic states of these structures and eventually can suppress the ABE in quantum rings.[9,11,24,25] In order to study electron states in ring-shaped systems, free of impurities and pinning centers, Dyugaev *et al.*[26] proposed an experimental apparatus consisting of a thin film of liquid helium over a substrate with a metal ring placed below, producing an electron confinement in the shape of a ring. Since its confinement potential is electrostatic, the proposal was applied only in the limit where the lateral confinement could be approximated by a parabolic potential, when the ABE is achieved.[27,28]

In the present paper, we propose a geometrical ring-shaped electron confinement built by a liquid helium film suspended by a substrate, where the distance between the helium film surface and the substrate is large enough, such that the van der Waals effect is not important and subjected to external electric and magnetic fields. Considering a single electron problem, the paper is organized as follows. In Sec. II, we present the calculation of the helium film profile and calculate the lateral confining potential of the electron in the

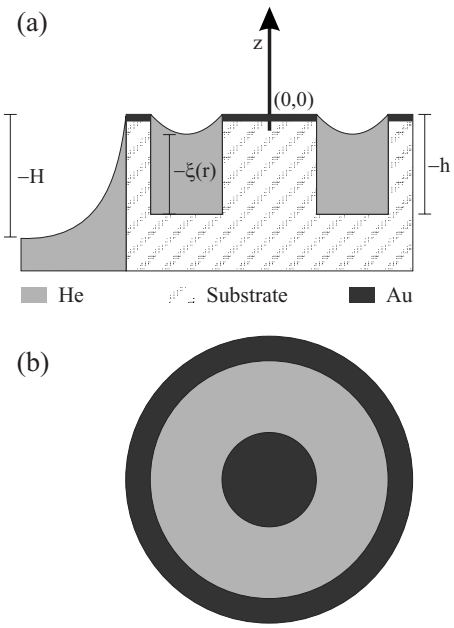

FIG. 1. (a) The cell transversal section of the helium film suspended over a ring-shaped substrate. (b) Top view of the system.

ring for various values of the external electric field, height of the bulk helium, and for different external radii of the ring. In Sec. III, we present the energy states of one electron subjected to the lateral confining potential, where we observe AB oscillations in the presence of a magnetic field. Finally, in Sec. IV, we present our conclusions.

II. HELIUM FILM PROFILE AND CONFINEMENT POTENTIAL

The system is schematically shown in Fig. 1 and consists of superfluid helium that flows from bulk liquid helium at a given level $z=-H$ and fills a ring-shaped structure of height h, produced on a substrate, due to the action of capillary forces. The ring has internal and external radii $r_<$ and $r_>$, respectively, where electrons over the liquid helium surface will be confined.

In order to obtain the helium profile suspended over the circular substrate, we calculate the pressure difference between the suspended film over the substrate and the free surface of the bulk liquid at height $-H$, as shown in Fig. 1, that produces a curved surface, due to the surface tension α.[29] We use the fact that in equilibrium, the chemical potential per unit mass is the same everywhere on the surface of the helium.[30] Thus, the work necessary to deform the surface by $-\delta\xi$ from its equilibrium position, $z=0$, is given by[29]

$$\delta W = \int (p_1 - p_2)\delta\xi df + \alpha\delta f, \tag{1}$$

where df is the surface element, p_1 the pressure on the free surface of the bulk, and p_2 the pressure inside the suspended helium film. The first term in Eq. (1) corresponds to the volume variation, whereas the second one corresponds to the surface area variation associated with this volume variation. In accordance with Fig. 1, the surface of the helium film is described by $z(r)=\xi(r)-h$ and we assume that $\xi(r)$ is small everywhere, i.e., that the surface deviates only slightly from the plane $z=0$. Then, as the surface has angular symmetry, the surface area is given by

$$f = 2\pi \int_{r_<}^{r_>} r\sqrt{1+\left(\frac{d\xi}{dr}\right)^2}\, dr, \tag{2}$$

where $r_<$ and $r_>$ are the internal and external radii of the ring. Since we assumed $\xi(r)$ to be small, we can expand Eq. (2) and obtain

$$f \simeq 2\pi \int_{r_<}^{r_>} \left[1+\frac{1}{2}\left(\frac{d\xi}{dr}\right)^2\right] r dr, \tag{3}$$

such that the variation δf is given by

$$\delta f = 2\pi \int_{r_<}^{r_>} \frac{d\xi}{dr}\frac{d\delta\xi}{dr} r dr. \tag{4}$$

Integrating Eq. (4) by parts, we find

$$\delta f = -2\pi \int_{r_<}^{r_>} \left(\frac{d^2\xi}{dr} + \frac{1}{r}\frac{d\xi}{dr}\right)\delta\xi r dr. \tag{5}$$

Inserting Eq. (5) into Eq. (1) and taking $\delta W=0$ (thermodynamic equilibrium condition), we obtain the pressure difference at the helium film that is suspended by the substrate,

$$p_2 = p_1 - \alpha\left(\frac{d^2\xi}{dr^2} + \frac{1}{r}\frac{d\xi}{dr}\right). \tag{6}$$

Knowing the pressures in and out of the ring, we can calculate the total chemical potential per unit mass in all regions, which is given by[30]

$$\mu = \frac{p}{\sigma} - sT + gz(r) - \frac{\gamma}{\sigma\xi^3(r)}, \tag{7}$$

where p is the pressure per unit mass, $\sigma=0.145$ g/cm^3 the helium density, $\gamma=9.5\times10^{-15}$ erg the van der Waals coupling constant of the helium substrate (assumed to be glass), s the specific entropy per unit mass, $gz(r)$ the potential energy per unit mass at height $z(r)$, $\xi(r)$ the thickness variation of the helium film, and g the gravity acceleration. Consequently, the total chemical potential per unit mass of the free surface of the bulk liquid, at height $-H$, is given by

$$\mu_1 = \frac{p_1}{\sigma} - sT - gH, \tag{8}$$

and the chemical potential of the suspended liquid helium film by the substrate is given by

$$\mu_2 = \frac{p_2}{\sigma} - sT + gz(r) - \frac{\gamma}{\sigma\xi^3(r)}, \tag{9}$$

where $z(r)=\xi(r)-h$. In thermodynamic equilibrium, we have $\mu_1=\mu_2$. Using Eqs. (6)–(9), we obtain

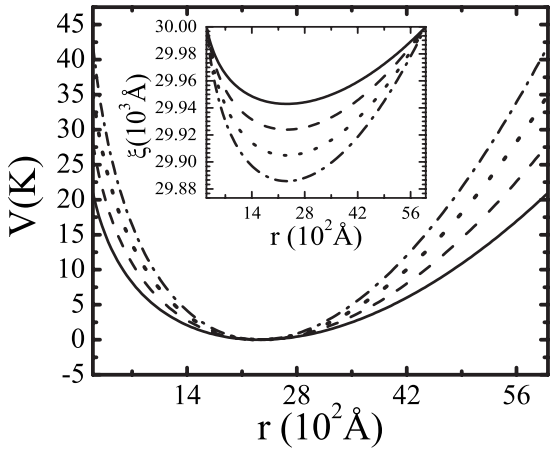

FIG. 2. The lateral confining potential of an electron in the ring as a function of the radius for various values of H. The solid, dashed, dotted, and dot-dashed curves correspond to $H=3$, 4, 5, and 6 cm, respectively. In the inset, we show the corresponding helium film profile.

$$\frac{d^2\xi(r)}{dr^2}+\frac{1}{r}\frac{d\xi(r)}{dr}=\frac{\sigma g}{\alpha}[\xi(r)-h+H]-\frac{\gamma}{\alpha\xi^3(r)}, \quad (10)$$

which describes the profile of the liquid helium film in the ring, where $\alpha=0.378$ erg/cm[22] is the liquid helium surface tension. Similar equation was obtained in Ref. 16 for the liquid helium film profile in channels.

Since the bonding energy of the electron over the liquid helium is around 8 K,[31] to confine the electron inside the ring of the suspended helium film, it is necessary to add an external electric field E_p in the z direction. The lateral confining potential due to the presence of this external electric field is given by

$$V(r)=\int_{\bar{r}}^{r} dr' eE_p\frac{dz(r')}{dr'}, \quad (11)$$

where $\bar{r}$ is the lowest point at the surface of the suspended helium film. Since $z(r)=\xi(r)-h$, the integral in Eq. (11) is straightforward and the lateral confining energy potential of the electron in the ring is given by

$$V(r)=eE_p[\xi(r)-\xi(\bar{r})]. \quad (12)$$

We solved Eq. (10) numerically, considering a ring with fixed internal radius $r_<=200$ Å and height $h=3\times10^4$ Å, and calculated the lateral confining energy potential of the electron as a function of the radius for different values of the bulk liquid helium level H, ring external radius $r_>$, and external electric field.

Considering an external ring of radius $r_>=6000$ Å and an external electric field $E_p=3$ kV/cm, we show in Fig. 2 the lateral confining potential as a function of the radius for several values of H. The inset shows the corresponding helium film profile. First, we notice that the helium film profile becomes deeper with increasing H and, consequently, the lateral confining energy potential also increases, with energy values up to 35 K. As can be seen, the lateral confinement

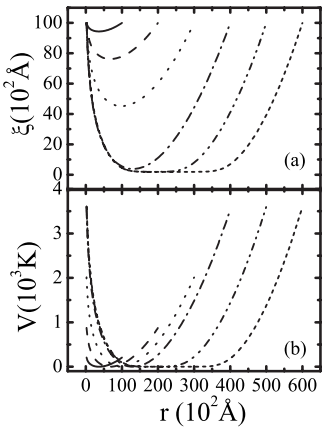

FIG. 3. (a) Helium film profile in the ring for several values of the external radius. The solid, dashed, dotted, dash-dotted, dash-dot-dotted, and short-dashed curves correspond to external radii $r_>=1$, 2, 3, 4, 5, and 6×10^4 Å, respectively. (b) The lateral confining potential of an electron in the ring for the same conditions.

potential is asymmetrical, such that only very close to the region of the lowest point at the surface of the suspended helium film the parabolic approximation is valid.

In Fig. 3(a), we show the helium film profile for several values of the external radius. In Fig. 3(b), we show the confinement potential for the same external radius. These results were obtained for a bulk helium level of $H=10$ cm, internal radius $r_<=200$ Å, height $h=10^4$ Å, and an external electric field of $E_p=3$ kV/cm. We note that the liquid helium profile becomes deeper when the external radius increases. Again, the lateral confinement is asymmetric and can reach values of the order of 4000 K, allowing electron confinement inside the ring for realistic values of the geometrical parameters. The parabolic approximation of the confinement potential is valid for values up to $r_>=4.6\times10^4$ Å. In Fig. 4, we show the frequency (ω_0) associated with each parabolic potential approximation shown in Fig. 3(b), and in the inset, we present the minimum value of the liquid helium film profile

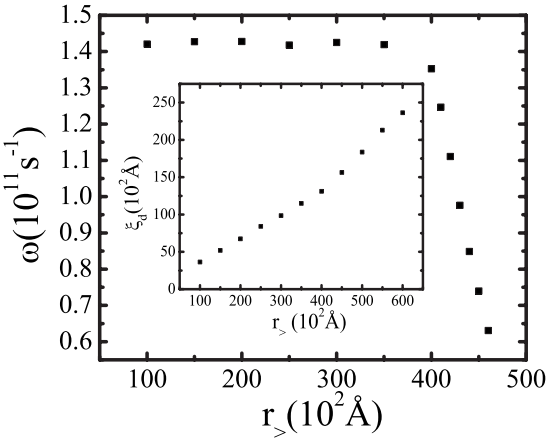

FIG. 4. The parabolic confining frequency versus $r_>$. In the inset, the minimum value of the liquid helium film profile (ξ_d) as a function of the external radius. The parameters used here are the same as in Figs. 3(a) and 3(b).

(ξ_d) as a function of the external radius. We observe that, for an external radius up to $r_>=3.5\times10^4$ Å [$r_>$(lim)], ξ_d is a linear function and ω_0 is a constant. For values of the external radius greater than $r_>$(lim) and below $r_>$(max)$=r_>$ $=4.6\times10^4$ Å, there is a transition such that the curve ξ_d versus $r_>$ is still linear but changes its slope and the frequency ω_0 decreases. For values above $r_>$(max), a second transition occurs, such that the parabolic approximation is no longer valid and the liquid helium profile becomes flat and behaves as a van der Waals film. The parameters used here for the liquid helium film are far below the first transition.

III. HAMILTONIAN MODEL AND ELECTRON ENERGY LEVELS

Considering now the system subjected to external electric and magnetic fields applied in the z direction, the Hamiltonian is given by

$$H=\frac{1}{2m}\left(\vec{p}-\frac{e}{c}\vec{A}\right)^2+V(r), \tag{13}$$

where $V(r)$ is given by Eq. (12). For an applied magnetic field perpendicular to the ring plane, i.e., $\vec{B}=B\hat{z}$, the symmetric gauge $\vec{A}=1/2Br\hat{\theta}$ is taken for the vector potential, which leads to the following form for the Schrödinger equation:

$$\left\{-\frac{\hbar^2}{2m}\left[\frac{1}{r}\frac{\partial}{\partial r}\left(r\frac{\partial}{\partial r}\right)+\frac{1}{r^2}\frac{\partial^2}{\partial\theta^2}\right]-\frac{i}{2}\hbar\omega_c\frac{\partial}{\partial\theta}+\frac{1}{8}m\omega_c^2r^2+V(r)\right\}\Psi(r,\theta)=E\Psi(r,\theta), \tag{14}$$

where $\omega_c=eB/mc$. Taking the solution in θ given by $e^{il\theta}/\sqrt{2\pi}$, where $l=0,\pm1,\pm2,\ldots$. is the angular momentum quantum number, the radial part of the Schrödinger equation will be[32]

$$\left\{-\frac{\hbar^2}{2m}\frac{1}{r}\frac{\partial}{\partial r}\left(r\frac{\partial}{\partial r}\right)+\frac{l^2\hbar^2}{2mr^2}+\frac{l}{2}\hbar\omega_c+\frac{1}{8}m\omega_c^2r^2+V(r)\right\}R_{n,l}(r)=E_{n,l}R_{n,l}(r). \tag{15}$$

Again, considering a ring with fixed internal radius $r_<$ $=200$ Å and height $h=3\times10^4$ Å, we obtain the energy levels of the electron confined in the ring as a function of the external electric field, bulk liquid helium level H, and external magnetic field. Also, to solve numerically Eq. (15), we consider an infinity potential for the region $r_<=200$ Å which is a very good approximation, as can be seen from Figs. 2 and 3. This approximation does not change significantly our results since the electron wave function is already negligible for $r<r_<$.

Considering initially $B=0$, $H=5$ cm, and $r_>=2000$ Å, we obtain the electron energy levels [Eq. (15)] as a function of the external electric field (Fig. 5). We observe that the number of bound states in the ring increases with the external electric field. This behavior is due to the fact that the lateral confining potential in the ring also increases with the external electric field. The line $(n,l)=(3,0)$ represents a bound state energy limit on the ring. Moreover, we note degenerate states in the crossing of the levels, for $E_p\simeq1.5$ kV/cm, $(n,l)=(1,\pm4)$ and $(2,\pm1)$, as well as for $(1,\pm4)$ and (2,0) for $E_p\simeq2.5$ kV/cm.

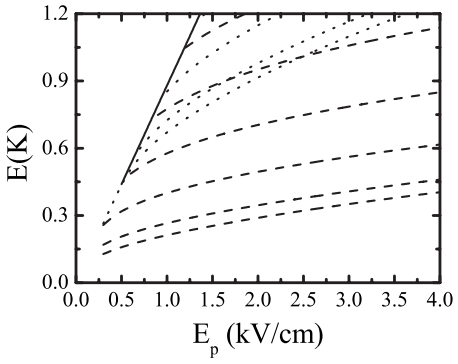

FIG. 5. Energy levels of the electron confined in the ring as a function of the external electric field. From bottom to top, the dashed, dotted, and solid curves correspond to energy levels $n=1(l=0,\pm1,\pm2,\pm3,\pm4,\pm5)$, $n=2(l=0,\pm1,\pm2)$, and $n=3(l=0)$, respectively.

Taking $r_>=6000$ Å and $E_p=3$ kV/cm, we obtain the energy levels of the electron confined in the ring as a function of the bulk liquid helium level (see Fig. 6). The results with $l=\pm1$ were not shown since they differ from the ones with $l=0$ by less than 10^{-2} K. We observe that the distance between the energy levels with n and $n+1$ increases with H, whereas the difference between energy levels with l and $l+1$ for a given n is constant, forming an energy band structure. The levels increase with H since the lateral confining potential increases with H, as shown in Fig. 2.

In Fig. 7, we show the energy levels as a function of the external radius with $B=0$, $E_p=3$ kV/cm, $h=3\times10^4$ Å, and $H=5$ cm. The numbers of bound electron levels increase for rings with larger radius. We also note crossing of energy levels for different values of n. Therefore, more degenerate states can be obtained when increasing the external radius. Again, an energy band structure is observed in the limit of large values of the external radius. Note that the energy levels do not go to zero near $r_>=10^4$ Å but remain constant. The reason for this remarkable result is that for this value of

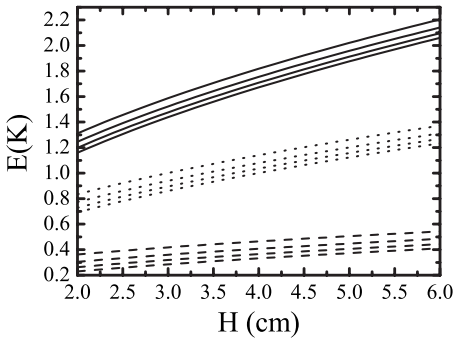

FIG. 6. Electron energy levels as a function of the bulk liquid helium level. The dashed, dotted, and solid curves correspond to levels $n=1$, 2, and 3, with $l=0$, ±2, ±3, and ±4 for each value of n, respectively.

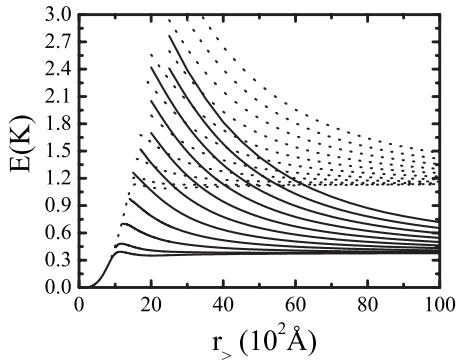

FIG. 7. Energy levels of the electron confined in the ring as a function of the external radius. The solid and dotted curves correspond to levels $n=1$ and 2, respectively, for increasing values of l, from $l=0$ up to $l=\pm 9$.

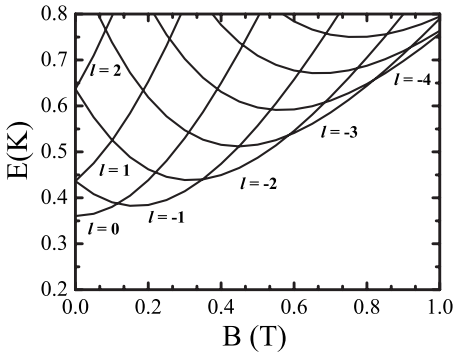

FIG. 8. Energy levels as a function of the external magnetic field. The curves are for $n=1$ and several different values of l.

the external radius, $H=5$ cm and $h=3\times10^4$ Å, the confining potential may be approximated by a parabola, with confining frequency $\omega_0\simeq10^{11}$ s^{-1}, which is constant up to $r_>(\max)\lessapprox 9\times10^5$ Å. For external radius larger than $r_>(\max)$, ω_0 decreases to zero since the helium film profile and the confining potential become flat. This is consistent with the results shown in Figs. 3 and 4.

In Fig. 8, we present the energy levels of the electron confined in the ring as a function of the external magnetic field for $r_>=1600$ Å, $E_p=3$ kV/cm, and $H=5$ cm. Notice that the magnetic field lifts the $-l,l$ degeneracy as expected. We observe that the ground state oscillates with magnetic field, showing the well known Aharonov-Bohm oscillations.[23] The present results shown are not limited, as the ones obtained by Dyugaev *et al.*,[26] to the weak-field limit.

IV. CONCLUSIONS

We obtained the lateral confining potential for an electron, subjected to external electric and magnetic fields, in a suspended helium film over a ring-shaped substrate. Considering realistic values for the geometrical parameters, we found that the parabolic potential approximation for the confinement potential has a very limited applicability. The energy levels tend to form an energy band structure, in the limit of high external electric field and large values of the outer ring radius. AB oscillations were found when a magnetic field is applied. Finally, this system can be used to study similar phenomena previously observed in quantum rings grown in semiconductor heterostructures, where geometrical imperfections and impurities are usually present, and the geometrical dimensions are an order of magnitude less than the one considered here.

ACKNOWLEDGMENTS

The authors thank the Conselho Nacional de Desenvolvimento Científico e Tecnológico (CNPq) and the Fundação Cearense de Apoio à Pesquisa (FUNCAP) for the financial support. This work was partially supported by the Flemish Science Foundation (FWO-Vl) and the EU-RTNetwork on "Surface electrons."

*acaramos@fisica.ufc.br
†andrey@fisica.ufc.br
‡gil@fisica.ufc.br
§francois.peeters@ua.ac.be

[1] W. T. Sommer, Phys. Rev. Lett. **12**, 271 (1964).
[2] M. Cole and M. H. Cohen, Phys. Rev. Lett. **23**, 1238 (1969).
[3] V. B. Shikin, Sov. Phys. JETP **31**, 936 (1970).
[4] F. M. Peeters, in *The Physics of Two-Dimensional Electron Gas*, edited by J. T. Devreese and F. M. Peeters (Plenum, New York, 1987).
[5] *Two-Dimensional Electron Systems on Helium and the other Cryogenic Substrates*, edited by E. Y. Andrei (Kluwer Academic, Dordrecht, 1997).
[6] B. Szafran and F. M. Peeters, Europhys. Lett. **12**, 271 (2005); B. Molnàr, P. Vasilopoulos, and F. M. Peeters, Appl. Phys. Lett. **85**, 612 (2004); P Földi, B. Molnàr, M. G. Benedict, and F. M. Peeters, Phys. Rev. B **71**, 033309 (2005).
[7] T. Kuroda, T. Mano, T. Ochiai, S. Sanguinetti, K. Sakoda, G. Kido, and N. Koguchi, Phys. Rev. B **72**, 205301 (2005), and references therein.
[8] Daniel Granados and Jorge M. Garcia, Appl. Phys. Lett. **82**, 2401 (2003).
[9] B. S. Monozon and P. Schmelcher, Phys. Rev. B **67**, 045203 (2003).
[10] L. G. G. V. Dias da Silva, S. E. Ulloa, and A. O. Govorov, Phys. Rev. B **70**, 155318 (2004).
[11] A. Bruno-Alfonso and A. Latgé, Phys. Rev. B **71**, 125312 (2005).
[12] Yu. Z. Kovdrya, Low Temp. Phys. **29**, 77 (2003).
[13] S. S. Sokolov, A. C. A. Ramos, and N. Studart, J. Phys.: Condens. Matter **12**, 7341 (2000).
[14] A. M. C. Valkering and R. W. van der Heidjen, Physica B **249–251**, 652 (1998); A. M. C. Valkering, J. Klier, and P. Leiderer, *ibid.* **284–288**, 172 (2000).
[15] S. S. Sokolov and N. Studart, Phys. Rev. B **51**, 2640 (1995).
[16] A. C. A. Ramos, O. G. Balev, and N. Studart, J. Low Temp. Phys. **138**, 403 (2005).

[17] D. Coimbra, S. S. Sokolov, J. P. Rino, and N. Studart, J. Low Temp. Phys. **126**, 505 (2002).
[18] H. W. Choi, C. W. Jeon, C. Liu, I. M. Watson, M. D. Dawson, P. R. Edwards, R. W. Martin, S. Tripathy, and S. J. Chua, Appl. Phys. Lett. **86**, 021101 (2005).
[19] Boris S. Monozon, Mikhail V. Ivanov, and Peter Schmelcher, Phys. Rev. B **70**, 205336 (2004).
[20] T. Raz, D. Ritter, and G. Bahir, Appl. Phys. Lett. **82**, 1706 (2003).
[21] Z. Barticevic, M. Pacheco, and A. Latgé, Phys. Rev. B **62**, 6963 (2000).
[22] A. Lorke, R. J. Luyken, A. O. Govorov, J. P. Kotthaus, J. M. Garcia, and P. M. Petroff, Phys. Rev. Lett. **84**, 2223 (2000).
[23] Y. Aharonov and D. Bohm, Phys. Rev. **115**, 485 (1959).
[24] L. A. Lavenère-Wanderley, A. Bruno-Alfonso, and A. Latgé, J. Phys.: Condens. Matter **14**, 259 (2002).
[25] D. Gridin, A. T. I. Adamou, and R. V. Craster, Phys. Rev. B **69**, 155317 (2004).
[26] A. M. Dyugaev, A. S. Rozhavskii, I. D. Vagner, and P. Wyder, JETP Lett. **67**, 434 (1998).
[27] R. J. Warburton, C. Schaflein, D. Half, F. Bickel, A. Lorke, K. Karrai, J. M. Garcia, W. Schoenfeld, and P. M. Petroff, Nature (London) **405**, 926 (2000).
[28] A. Lorke, R. J. Luyken, A. O. Govorov, J. P. Kotthaus, J. M. Garcia, and P. M. Petroff, Phys. Rev. Lett. **84**, 2223 (2000); A. Lorke and R. J. Luyken, Physica B **256**, 424 (1998).
[29] L. Landau and E. Lifshitz, *Fluid Mechanics*, 2nd ed. (Pergamon, New York, (1987).
[30] D. R. Tilley and J. Tilley, *Superfluidity and Superconductivity*, 3rd ed. (IOP, Bristol, 1990).
[31] C. C. Grimes, Surf. Sci. **73**, 379 (1978).
[32] F. M. Peeters and V. A. Schweigert, Phys. Rev. B **53**, 1468 (1996).